



Active electron energy distribution function control in direct current discharge using an auxiliary electrode

I. V. Schweigert, I. D. Kaganovich, and V. I. Demidov

Citation: [Phys. Plasmas](#) **20**, 101606 (2013); doi: 10.1063/1.4823465

View online: <http://dx.doi.org/10.1063/1.4823465>

View Table of Contents: <http://pop.aip.org/resource/1/PHPAEN/v20/i10>

Published by the [AIP Publishing LLC](#).

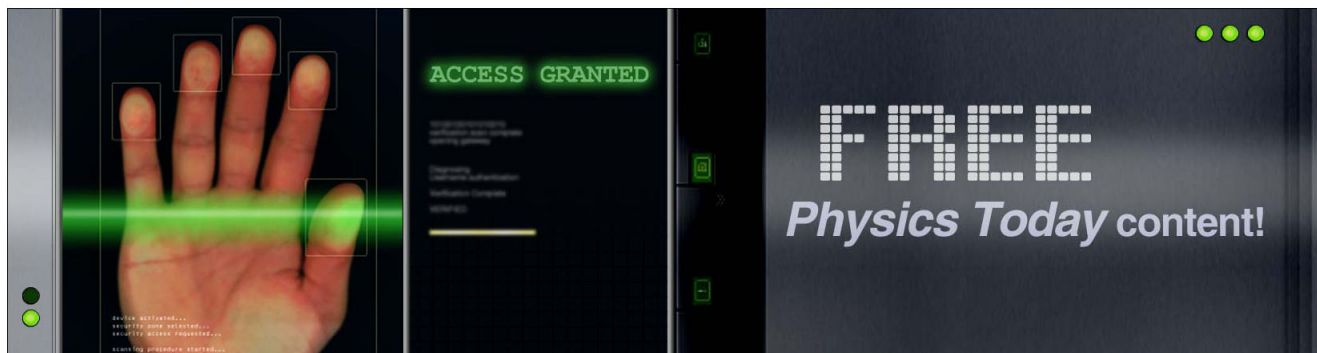
Additional information on Phys. Plasmas

Journal Homepage: <http://pop.aip.org/>

Journal Information: http://pop.aip.org/about/about_the_journal

Top downloads: http://pop.aip.org/features/most_downloaded

Information for Authors: <http://pop.aip.org/authors>



Active electron energy distribution function control in direct current discharge using an auxiliary electrode

I. V. Schweigert,^{1,2,a)} I. D. Kaganovich,³ and V. I. Demidov^{4,5}

¹*Institute of Theoretical and Applied Mechanics, Novosibirsk 630090, Russia*

²*George Washington University, Washington, DC 20052, USA*

³*Princeton Plasma Physics Laboratory, Princeton, NJ 08543, USA*

⁴*West Virginia University, Morgantown, WV 26506, USA*

⁵*St. Petersburg State University, St. Petersburg, Russia*

(Received 25 April 2013; accepted 18 July 2013; published online 10 October 2013)

The electron energy distribution functions are studied in the low voltage dc discharge with a constriction, which is a diaphragm with an opening. The dc discharge glows in helium and is sustained by the electron current emitted from a heated cathode. We performed kinetic simulations of dc discharge characteristics and electron energy distribution functions for different gas pressures (0.8 Torr–4 Torr) and discharge current of 0.1 A. The results of these simulations indicate the ability to control the shape of the electron energy distribution functions by variation of the diaphragm opening radius. © 2013 AIP Publishing LLC. [<http://dx.doi.org/10.1063/1.4823465>]

Low-pressure discharges are widely used as the plasma sources for a variety of plasma applications, including plasma processing, discharge lighting, sources for particle beams, and nanotechnology. The production of low-temperature plasmas with controllable parameters, including the plasma density, the electron temperature, and the electron and ion energy distribution functions is one of the critical challenges of modern plasma engineering.¹ Optimization of plasma parameters necessitates basic research with the main objective of developing sophisticated modeling capabilities to capture the key processes in the plasma and plasma–wall interactions.² The distinctive property of plasmas of these discharges is that such plasmas are always in a non-equilibrium state: the electrons are not in thermal equilibrium with the neutral species and ions, in view of the fact that the electron mean energy is typically much larger than the mean energy of the ions and neutrals. Moreover, the electrons are also not in thermodynamic equilibrium within their own ensemble, which results in a significant departure of the electron velocity distribution function (EVDF) from a Maxwellian EVDF—the EVDF may have a complex form and sometimes can be noticeably anisotropic. These non-equilibrium conditions make gas-discharge plasmas a remarkable tool for plasma applications, because they provide considerable freedom to choose optimal plasma properties. The theory on nonlocal electron kinetics was pioneered by Tsendin and described in his recent reviews and books.¹

In this paper, we study ways to produce and control electron energy distribution function making use of a constriction in the current channel. Previous experiments show that the narrow constriction in the dc discharge leads to the enrichment of the electron energy distribution with fast electrons (see, for example, Refs. 3–5). However, to the best of our knowledge, there was no detailed simulation study of this effect, which is the focus of this paper.

In this work, we study the means to control the formation of the electron energy distribution function (EEDF) in dc discharge with hot cathode. A diaphragm with an opening in the center is used to produce a constriction. The geometry and parameters of dc discharge were chosen to be identical with that of the experimental study reported in Ref. 6. The schematics of the device is shown in Fig. 1. The device is axi-symmetrical structure with disk cathode and anode with 0.5 cm and 1.4 cm radii, respectively, and a conical side-wall electrically connected with the cathode.⁶ The inter-electrode distance is 1.1 cm. The diaphragm with a hole in the center is inserted near the anode at the distance of 0.1 cm from the anode. The width of diaphragm is 0.2 cm. The thermo-emission of electrons from the heated cathode maintains the glow of dc discharge.

In helium, at gas pressure $P = 1$ Torr, the electron inelastic collision free path $\lambda_i \approx 1$ cm. For our applied voltage ($U_a = 30$ V), the cathode sheath length l_{sh} is approximately 0.1 cm, and consequently, $\lambda_i \gg l_{sh}$. This gas pressure was taken in the previous experiments and in recent simulations to ensure non-local character of the electron energy distribution function. The electrons emitted from cathode gain energy crossing the cathode-potential-fall region and reach the bulk plasma practically without energy losses. Moreover, special geometry of device also enhances the nonlocal properties of EEDF. The presence of constriction initiates an increase of electrical potential in front of the opening. At this position, the electrons are accelerated to the anode direction. The peak of the electron energy as well as the peak of ionization rate are observed in the center of the opening where the plasma is quasi-neutral, and the electrical fields are very small. This is a manifestation of the non-local regime of electron transport. The EEDF is not determined by a local strength of the electric field but the entire electric potential profile.¹

The elastic collision free path for electrons ($l_{el} = 0.1$ cm) is much less than the discharge gap ($d = 1.1$ cm). Therefore, the EVDF is nearly isotropic in the plasma bulk. In the pressure range below 7 Torr, the electron energy losses in elastic

^{a)}ischweig@itam.nsc.ru

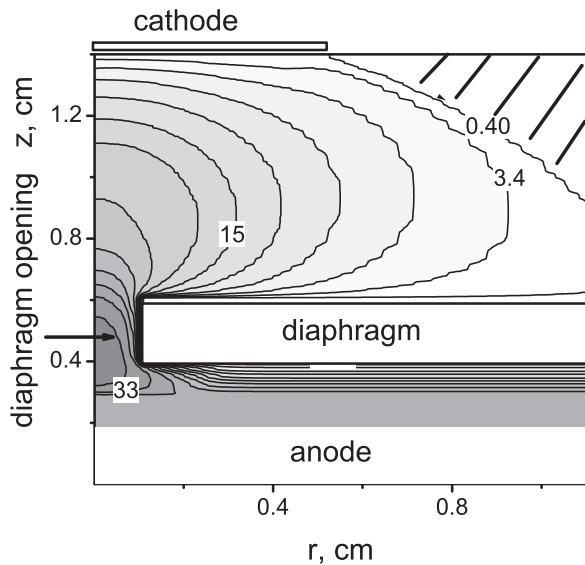


FIG. 1. Potential distribution (measured in Volts) for anode voltage $U_a = 30$ V, $j_{th} = 0.23$ A, $j_a = 0.1$ A, $P = 0.8$ Torr, and $r_d = 0.1$ cm.

collisions with He atoms are small⁶ compared to inelastic collision losses.

The electrons emitted from cathode have highest energy and maintain discharge by providing direct and step-wise ionization processes similar to the negative glow of dc discharges.¹ The electric field in the bulk plasma is weak and electrons produced by ionization have low energy compared with the electrons emitted from cathode. However, a small opening in the diaphragm can provide a potential drop in plasma comparable to the cathode fall. This potential drop can accelerate electrons toward anode and provide additional ionization source in the anode region. This study focuses on the non-local effect of electron kinetics and its employment for plasma formation and control.

We performed kinetic simulations of characteristics of dc discharge with a diaphragm in cylindrical geometry (the z axis is the axis of symmetry). The simulation set up of the device is shown in Fig. 1. We solve the Boltzmann equation for electron energy distribution function and the Boltzmann equation for ion energy distribution function, using the two dimensional particle-in-cell Monte-Carlo collision algorithm.⁷ We use the “leap-frog” difference scheme for electron motion, weighting scheme with linear-interpolation and null collision technique, as described in Ref. 7. We solved self-consistently the Boltzmann equations and Poisson equation for electrical potential distribution. The iterative method is used to obtain the steady-state solution.

This advanced method is widely used for simulation of dynamics of low gas pressure plasma with non-local regime of charged particle motion (see, for example, Refs. 8 and 9). The initial charged particle distributions were calculated with solving diffusion equation. We use a nonuniform grid for more accurate resolution of plasma parameters near the walls.

Electron kinetic processes included in simulation are elastic scattering on helium atoms, excitation of metastable states, and ionization of helium atoms. The ion collisional processes include the resonance charge exchange and elastic collisions with helium atoms. The ionization process includes the direct

ionization of He-atoms by electron impact and stepwise ionization of He-atoms in metastable state. Calculation of the distribution of He-atoms in metastable state requires a long simulation time taking into account long and slow accumulation of He-atoms in metastable state. We simplified simulation by assuming that when atoms are excited in metastable state, 18% of these events leads to ionization and the rest to deactivation by collisions with the walls. This corresponds to the rate of stepwise ionization measured in Ref. 10. This assumption allows us to reduce considerably simulation time and does not affect significantly the physical effects under consideration. Further refinement of simulation model can be done elsewhere.

The following discharge parameters are used: the anode voltage, $U_a = 30$ V, the diaphragm voltage, $U_d = 0$, and the discharge current $j_a = 0.1$ A. The gas pressure P ranges from 0.8 Torr to 4 Torr. The value of electron thermo-emission current j_{th} is adjusted to match the experimental value of the discharge current at anode, $j_a = 0.1$ A. The diaphragm opening radius is varied from 0.1 cm to 0.25 cm to study the effect of opening radius on plasma parameters.

An opening causes considerable modification of the potential profile, so that a localized maximum of the potential is formed in the opening. The formation of the maximum of the potential was observed in the earlier experiments in Refs. 4–6, and 11 and is reproduced in our simulations as shown in Fig. 1. The electrical field in front of the opening accelerates electrons and focuses their trajectories toward the opening. The focusing effect provides the continuity of discharge current from plasma bulk to the narrow channel in the opening. Behind the diaphragm, the electrons are decelerated, but not defocused, and the radius of the electron current spot on the anode remains approximately equal to the radius of the opening. This is probably because the distance between diaphragm and anode is sufficiently small.

We investigated modifications of plasma parameters due to variation of the opening radius. The electrical potential and electron density profiles are shown in Fig. 2 for different radii of the opening. The potential in front of the opening rises for all cases. For the smallest radius, $r_d = 0.1$ cm, the potential bump is maximal (about 11 eV). For the largest radius, $r_d = 0.25$ cm, the opening does not affect considerably the plasma parameters. For this case, the electron density in the opening is even lower than in bulk plasma. The reduction of the opening radius leads to increase of the plasma density over the entire device volume and formation of a peak of plasma density inside of the opening.

This peak of plasma density in the opening is formed (see Fig. 2(b)) due to enhanced ionization and electrostatic confinement effect. The electrons are trapped inside the opening by the potential bump from the cathode side and side-wall potential of diaphragm. This potential fall near the diaphragm surface is characterized with the positive charge distribution, $(n_r - n_e)$, shown in Fig. 3. For this case, the potential fall at $z = 0.5$ cm in radial direction is equal to 35 V and the potential barrier from cathode side is 11 V. As seen in Fig. 1, the potential fall near the diaphragm at 0.6 cm $< z < 0.7$ cm and $r > r_d$ is identical to the cathode fall; therefore, the fast electrons can reach the diaphragm surface. However, the fast electrons after an inelastic collision are trapped

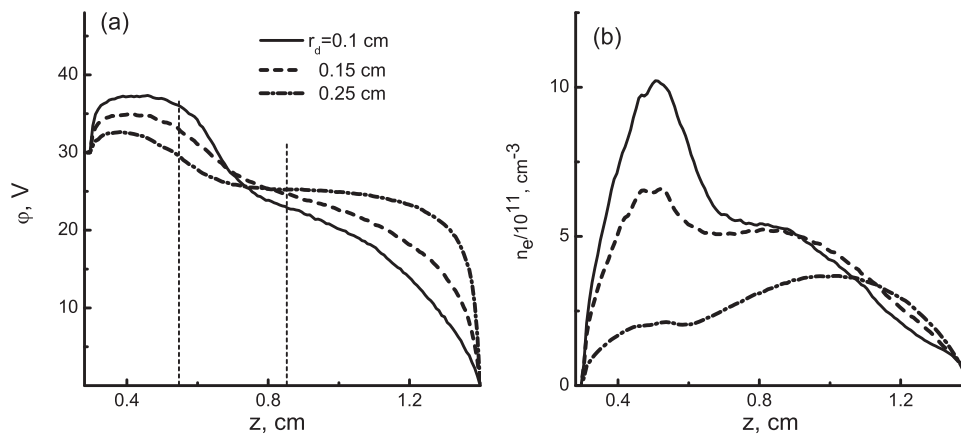


FIG. 2. Potential (a) and electron density (b) distributions at $r = 0$ for different radii of the opening, $r_d = 0.1$ cm ($j_{th} = 0.23$ A), 0.15 cm ($j_{th} = 0.157$ A), and 0.25 cm ($j_{th} = 0.1$ A), $P = 0.8$ Torr, $j_a = 0.1$ A. Vertical lines show the place of EEDFs calculation discussed below.

between cathode, diaphragm, and wall and can escape from discharge volume only through the opening.

The thermo-emission current j_{th} maintains the discharge glow and determines the value of discharge current j_a . To provide the given value of discharge current for different opening radii and gas pressures, we adjust j_{th} for each particular case. We found that for all cases the thermo-emission current is larger than the discharge current, i.e., $j_{th}/j_a > 1$. For smaller r_d and P , the ratio j_{th}/j_a increases, whereas for larger r_d and P the discharge current becomes approximately equal to the thermo-emission current. For example, for smaller $r_d = 0.1$ cm and $P = 0.8$ Torr, the discharge current of 0.1 A is sustained with $j_{th} = 0.25$ A, i.e., $j_{th}/j_a = 2.5$. Whereas for higher gas pressure case ($P = 4$ Torr, $r_d = 0.1$ cm) and for larger opening radius case ($r_d = 0.25$ cm, $P = 0.8$ Torr), the same discharge current is sustained with $j_{th} = 0.25$ A ($j_{th}/j_a = 1$).

Figures 4 and 5 depict variation of the EEDF with the opening radius for the cases shown in Fig. 2. The vertical

lines in Fig. 2 denote z -coordinates of calculated EEDFs. Fig. 4 shows the EEDFs for the case of $r_d = 0.25$ cm. The EEDF calculated at $z = 0.85$ cm (in front of the opening) has two peaks. First peak at $\varepsilon_e = 23$ eV corresponds to electrons which gain energy within cathode potential fall (23 V). The second peak at $\varepsilon_e \approx 3$ eV is associated with the electrons emitted from cathode that first gain energy within cathode potential fall and then lose 20 eV in single inelastic collision. The EEDF calculated in the center of the opening ($z = 0.55$ cm) is replica of the EEDF at $z = 0.85$ cm with some shift over the energy axis. This shift appears due to the electrons crossing the potential bump between $z = 0.55$ cm and $z = 0.85$ cm. They gain an additional energy which is about 3.5 eV for $r_d = 0.25$ cm.

Reducing the opening radius initiates the increase of the potential bump, and consequently, electron energy inside of the opening. As seen in Fig. 5, the high energy part of EEDFs is considerably enriched for smaller radii, $r_d = 0.15$ cm and 0.1 cm, in comparison with Fig. 4. Figure 5(a) shows the EEDFs in bulk plasma. There the peak of fast electrons for

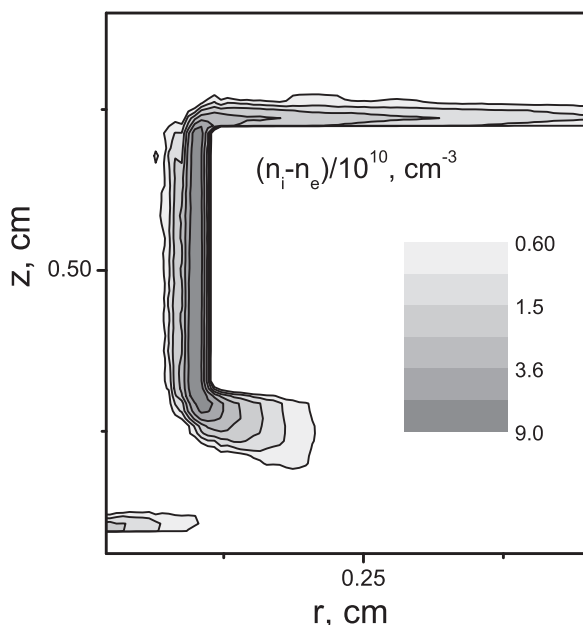


FIG. 3. Charge ($n_i - n_e$) distribution measured in 10^{10} cm^{-3} around diaphragm surface for $P = 0.8$ Torr, $r_d = 0.1$ cm, $j_{th} = 0.23$ A, $j_a = 0.1$ A.

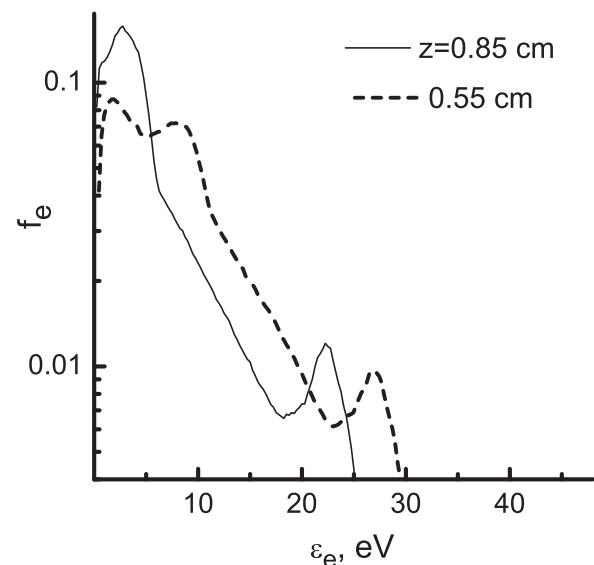


FIG. 4. Electron energy distribution function at $r = 0$ and $z = 0.85$ cm and $z = 0.55$ cm for $r_d = 0.25$ cm $P = 0.8$ Torr, $j_a = 0.1$ A ($j_{th} = 0.1$ A).

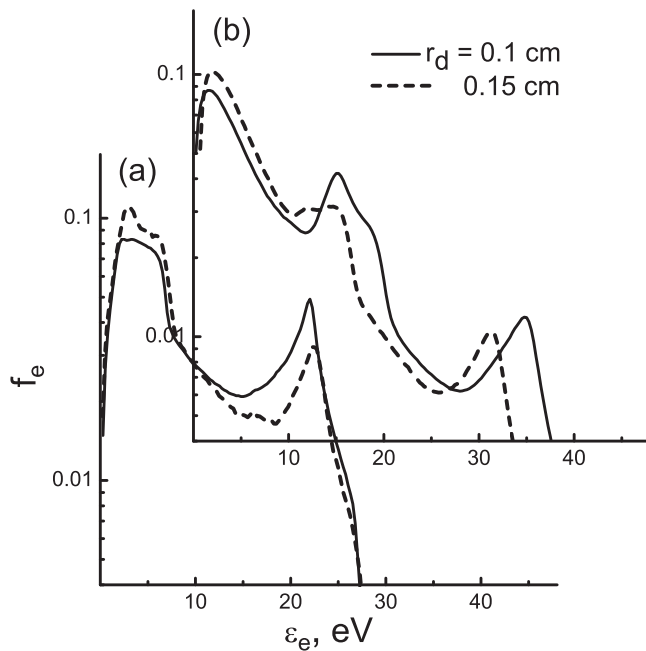


FIG. 5. Electron energy distribution function at $r = 0$ and $z = 0.85$ cm (a) and $z = 0.55$ cm (b) for $r_d = 0.1$ cm ($j_{th} = 0.23$ A), 0.15 cm ($j_{th} = 0.157$ A), $P = 0.8$ Torr, $j_a = 0.1$ A.

$r_d = 0.1$ cm is higher than the peak for $r_d = 0.15$ cm, which is explained by larger number of emitted electrons in the former case. We took the thermo-emission current $j_{th} = 0.23$ A for smaller $r_d = 0.1$ cm and $j_{th} = 0.16$ A for larger $r_d = 0.15$ cm to provide the same discharge current.

Figure 5(b) shows the EEDFs inside of the opening ($z = 0.55$ cm). Again each EEDF is replica of the EEDF shown in Fig. 5(a) with some shift $\delta\varepsilon$ over the energy axis. The maximum $\delta\varepsilon = 11$ eV is for $r_d = 0.1$ cm. This increase of the electron energy inside of the opening enhances the ionization rate that is followed by the increase of plasma density. For example, for $r_d = 0.1$ cm, the plasma density inside the opening is 5 times higher compared to the case of $r_d = 0.25$ cm.

With increasing gas pressure, the electron collision frequency rises, diffusion towards walls slows down and the ion loss frequency becomes smaller. This leads to the rise of

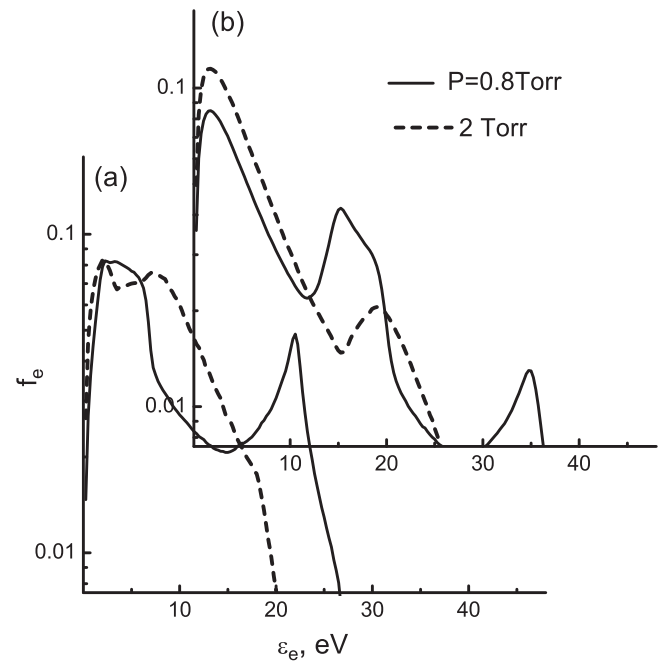


FIG. 7. Electron energy distribution function at $r = 0$ and $z = 0.85$ cm (a) and $z = 0.55$ cm (b), $P = 0.8$ Torr ($j_{th} = 0.23$ A) and $P = 2$ Torr ($j_{th} = 0.136$ A), for $r_d = 0.1$ cm, $j_a = 0.1$ A.

plasma density as evident in Fig. 6. Notice that for $P = 2$ Torr, the cathode fall voltage is less than 20 eV, which is the atom excitation and ionization threshold. Therefore, no excitation and ionization occurs in the volume between cathode and diaphragm. Thus, the ionization only takes place in front of the opening, but this ionization rate is sufficient to maintain 0.1 A discharge current on the anode.

The modification of the EEDF with increasing gas pressure is shown in Fig. 7. For higher gas pressure ($P = 2$ Torr), the energy losses in elastic and inelastic collisions become more frequent; therefore, the EEDF peak corresponding to fast electrons emitted from cathode disappears. Nevertheless, within the opening for $P = 2$ Torr, we still observe a group of high energy electrons with the ionization capability.

In conclusion, we have studied EEDF formation in the low voltage dc discharge sustained by the electron current

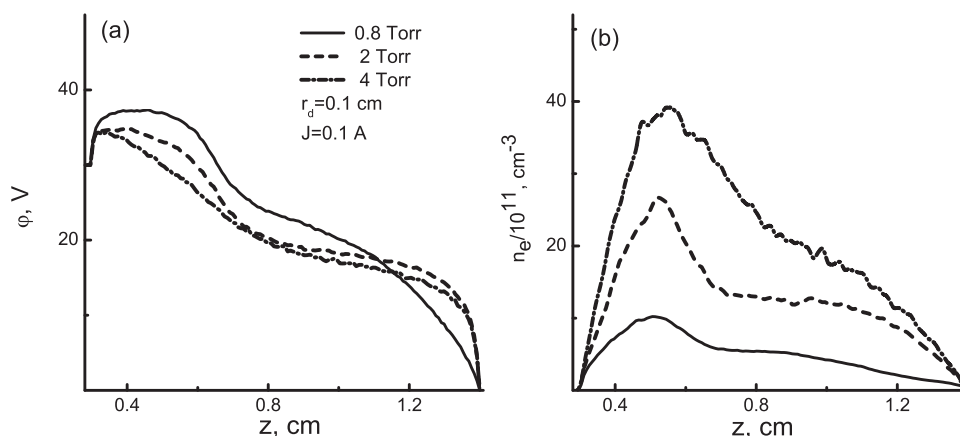


FIG. 6. Potential (a) and electron density (b) distributions at $r = 0$ for gas pressures $P = 0.8$ Torr ($j_{th} = 0.23$ A), 2 Torr ($j_{th} = 0.136$ A), and 4 Torr ($j_{th} = 0.1$ A), $r_d = 0.1$ cm, $j_a = 0.1$ A.

emitted from a heated cathode. A diaphragm with an opening in the center was placed at a certain distance from the anode to restrict the current channel. The EEDF formation was strongly affected by the diaphragm. The kinetic PIC MCC simulations of plasma parameters in the dc discharge in helium showed that the radius of the diaphragm opening is the key parameter that affects the shape of EEDFs. The decrease of the opening radius yields the increase of the potential drop near the opening needed to provide the current continuity. The simulations were carried out for the gas pressure ranged from 0.8 Torr to 4 Torr, for the discharge current of 0.1 A and for the opening radii, 0.1 cm-0.25 cm. In case of the opening radii, 0.1 cm-0.15 cm, the insertion of the diaphragm led to formation of the strong peak of fast electrons which were responsible for strongly enhanced excitation and ionization rate in the opening region.

One of authors (I. V. Schweigert) was supported by the RFBR Project No. 12-02-00854. Another author, V. I.

Demidov, was supported by the DOE OFES (Contract No. DE-SC0001939) and SPbGU.

- ¹L. D. Tsendin, "Electron kinetics in glows—From Langmuir to the present," *Plasma Sources Sci. Technol.* **18**, 014020 (2009); L. D. Tsendin, "Nonlocal electron kinetics in gas discharge," *Plasma Phys. Usp.* **201**, 501 (2010); A. A. Kudryavtsev, A. S. Smirnov, and L. D. Tsendin, *Physics of Glow Discharges* (LAN, 2010) (in Russian).
- ²I. D. Kaganovich, V. I. Demidov, S. F. Adams, and Y. Raitses, *Plasma Phys. Controlled Fusion* **51**, 124003 (2009).
- ³M. A. Abroyan, V. I. Demidov, Yu. M. Kagan, and B. P. Lavrov, *Opt. Spectrosc.* **39**, 12 (1975).
- ⁴B. P. Lavrov and V. Ya. Simonov, *J. Vestn. LGU* **16**, 13 (1984); in Proceedings of Conference on Gas Discharges, Kiev (1986), p. 443 (in Russian).
- ⁵V. Godyak, R. Lagushenko, and J. Maya, *Phys. Rev. A* **38**, 2044 (1988).
- ⁶V. I. Demidov, C. A. DeJoseph, Jr., and V. Ya. Simonov, *Appl. Phys. Lett.* **91**, 201503 (2007).
- ⁷C. K. Birdsall and A. B. Langdon, *Plasma Physics via Computer Simulation* (McGraw-Hill, New York, 1985).
- ⁸I. V. Schweigert *et al.*, *Plasma Source Sci Technol.* **20**, 015011 (2011).
- ⁹I. V. Schweigert and A. L. Alexandrov, *IEEE Trans. Plasma Sci.* **33**, 615 (2005).
- ¹⁰V. I. Demidov *et al.*, *J. Tech. Phys.* **59**, 55 (1989).
- ¹¹M. N. Shoenhuber, *Z. Angew. Phys.* **15**, 454 (1963).